

Evolution of microstructure and electrochemical corrosion characteristics of cold compacted magnesium

Vývoj mikrostruktury a elektrochemických korozních charakteristik práškového hořčíku lisovaného za studena

Březina M.¹, Doležal P.^{1,2}, Krystýnová M.¹, Minda J.¹, Zapletal J.², Fintová S.¹, Wasserbauer J.¹

¹ Brno University of Technology, Faculty of Chemistry, Czech Republic

² Brno University of Technology, Faculty of Mechanical Engineering, Czech Republic

E-mail: xcbrezinam@fch.vutbr.cz

The main advantage of magnesium and its alloys is high specific strength and biocompatibility. A modern approach to magnesium-based materials preparation is powder metallurgy. This technique allows preparation of new materials with a unique structure, chemical composition, and controlled porosity. In this study, cold compaction of magnesium powder was studied. Magnesium powder of average particle size of 30 μm was compacted applying pressures of 100 MPa, 200 MPa, 300 MPa, 400 MPa and 500 MPa at laboratory temperature. Influence of compacting pressure was studied with microstructural and electrochemical corrosion characteristics analysis. The resulting microstructure was studied in terms of light and electron microscopy. Obtained electrochemical characteristics were compared with those of wrought magnesium. Compacting pressure had a significant influence on microstructure and electrochemical characteristics of prepared bulk magnesium. With the increase in compaction pressure, the porosity decreased. Compacting pressures of 300 MPa, 400 MPa and 500 MPa led to the similar microstructure of the prepared material. Polarization resistance of compacted magnesium was much lower and samples degraded faster when compared to wrought magnesium. Also, the corrosion degradation mechanism changed due to the microstructural differences between the material states.

Hlavní výhodou hořčíku a jeho slitin je vysoká specifická pevnost a biokompatibilita. Moderní metodou přípravy hořčíkových materiálů je prášková metalurgie. Tato metoda umožňuje přípravu nových materiálů s unikátní strukturou, chemickým složením a řízenou porositou. V této studii byl zkoumán objemový hořčíkový materiál připravený lisováním za studena. Hořčíkový prášek o střední velikosti částic 30 μm byl lisován za laboratorní teploty tlakem 100 MPa, 200 MPa, 300 MPa, 400 MPa a 500 MPa. Byl studován vliv lisovacího tlaku na mikrostrukturu a elektrochemické vlastnosti připravených materiálů. Výsledná mikrostruktura byla studována pomocí světelné a elektronové mikroskopie. Elektrochemické charakteristiky byly srovnány s vlastnostmi tvářeného hořčíku. Lisovací tlak měl zásadní vliv na mikrostrukturu a elektrochemické vlastnosti připravených objemových materiálů. Se zvyšujícím se tlakem docházelo ke snižování porozity, vzorky připravené tlakem 300 MPa, 400 MPa a 500 MPa vykazovaly stejnou mikrostrukturu. Polarizační odpor připravených objemových materiálů byl mnohem nižší a vzorky degradovaly rychleji v porovnání s tvářeným hořčíkem. Došlo také ke změně charakteru degradace vlivem rozdílné mikrostruktury vzorků.

INTRODUCTION

Powder metallurgy of magnesium and its alloys is nowadays widely studied technology as it has great potential of producing new lightweight construction materials as well as new perspective biomedical materials. Magnesium based composites, porous magnesium materials and magnesium alloys are mostly used in aerospace and automotive industry and also in medicine. Most common powder metallurgy technologies are cold pressing and sintering, hot pressing, isostatic pressing and

spark plasma sintering. The microstructure of materials prepared with these technologies can be subsequently modified using intensive plastic deformation methods such as extrusion, equal channel axial pressing (ECAP) and high-pressure torsion (HPT). Using these methods, hardness and strength of materials can be maximized [1-5].

Wide area of applications in aerospace and automotive industry of bulk magnesium materials is due to their high specific strength. The general approach to increase the strength of metallic materials is the reduction

in grain size. This can be easily achieved using powder metallurgy followed by intensive plastic deformation techniques (extrusion, ECAP, HPT). This can be combined with solid solution strengthening of alloying elements and adding hard inorganic particles to powder mixture to produce magnesium based composites [6-10].

Low corrosion resistance of magnesium can be in special applications an advantage, as biodegradability of magnesium is in other words corrosion of magnesium in body fluids. Magnesium degrades into nontoxic products, and moreover, these products can enhance regeneration of damaged tissue. This provides a great advantage to conventional titanium or ceramic implants, which cannot degrade in the body and have to be removed. Polymer-based implants also undergo biodegradation, but they have much lower strength compared to magnesium-based materials. Magnesium itself, however, degrades too rapidly, which causes rapid evolution of hydrogen and swift decrease in mechanical properties. For improvement of rapid degradation calcium and zinc are added as alloying elements and hydroxyapatite or fluorapatite are added as particle filler in magnesium based composites [11, 12].

Materials with controlled porosity fully compressed materials and materials with unique structure and chemical composition which could not be prepared using conventional casting methods are easily prepared via powder metallurgy. Another advantage of powder metallurgy is an almost waste-free fabrication of precise products. In general powder metallurgy process consists of pressing a prepared mixture of powders into a mould of precise dimensions. During compaction, metal particles are deformed and begin to connect to each other and cold welds are created. However, compacted product (green compact) has low strength and needs to be sintered into a final product. Sintering is a process of solid state connection of particles via diffusion. The

advantage of this process is better control of composition throughout the whole body of prepared material and limited segregation of elements [13-15].

Magnesium based powder metallurgy alloys and composites are widely studied, however, only a few studies focus [16, 17] on properties of bulk magnesium prepared by powder metallurgy and influence of high plastic deformation techniques. Therefore in this study, we focus on properties of bulk magnesium prepared via cold compaction from the point of microstructure and electrochemical corrosion properties.

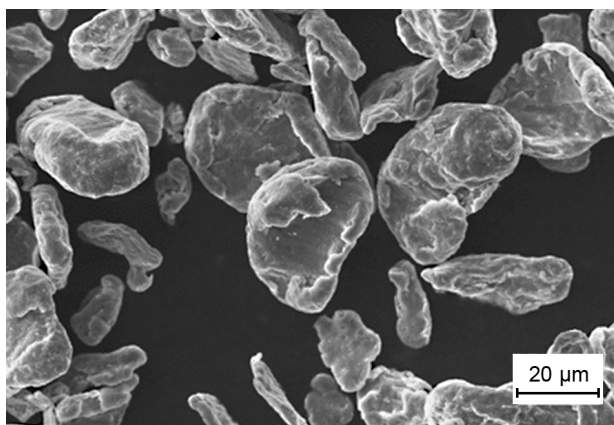
EXPERIMENTAL MATERIAL AND PROCEDURES

Base material

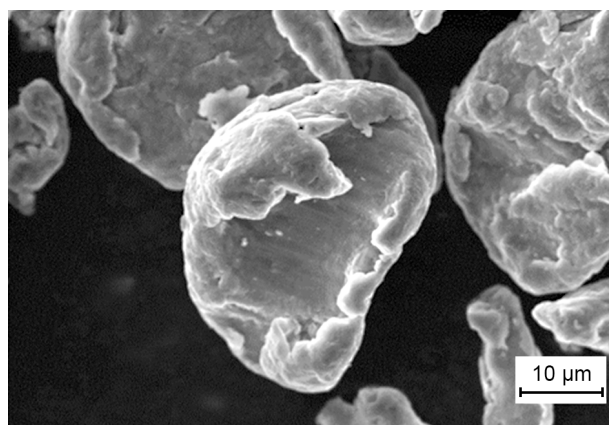
Magnesium powder used in this study (Fig. 1) was irregularly shaped with the average particle size of approximately 30 μm . The purity of base material was 99.8 % as declared by supplier Goodfellow, however, an oxide layer was found on the surface of powder particles using scanning electron microscope (SEM, ZEISS EVO LS 10) and energy dispersive spectroscopy (EDS). This layer of magnesium oxide is to be expected on the surface of magnesium and it was probably present on the particles from the powder preparation.

Experimental procedure

For metallographic and electrochemical analysis cylindrical compacts with 5 mm in height and 20 mm in diameter were prepared by cold compaction. 2.7 g of magnesium powder was inserted into steel die and compacted applying different uniaxial pressures; 100 MPa, 200 MPa, 300 MPa, 400 MPa and 500 MPa. Compaction was carried out at laboratory temperature using Zwick



a) powder morphology and size distribution / morfologie distribuce velikostí prášku



b) detail of the particle shape / detail tvaru práškových částic

Fig. 1. Magnesium powder, SEM
Obr. 1. Hořčikový prášek, SEM

Z250 Allround-Line machine equipped with sensitive extensometer MultiXtens set between pressing plates. Preparation of the magnesium powder into the die for compaction was carried out under nitrogen atmosphere to avoid further contamination of the powder by oxygen.

Metallographic analysis

The microstructure of prepared samples (compacts) was studied on cross-section using scanning electron microscope (SEM, ZEISS EVO LS 10) and light microscope (LM, Zeiss Axio Observer Z1m). Samples were mold into a polymeric resin at room temperature, ground and polished according to the standard procedure of metallographic samples preparation. The porosity of the compacted material was calculated from sample dimensions and weight.

Electrochemical analysis

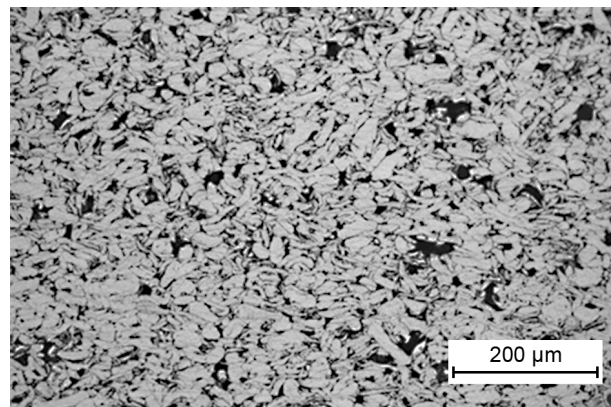
Potentiostatic electrochemical impedance spectroscopy was used as a method to characterize the prepared magnesium based samples electrochemical corrosion characteristics. Three electrode cell was used for the measurement with Pt electrode as the counter electrode, calomel electrode as the reference electrode and the sample (1 cm² exposed area) served as the working electrode. Sample surface was ground using 4000 sand paper and rinsed with isopropanol. Measurements were carried out in 0.9 % NaCl solution. Used frequency range was from 100 kHz to 10 MHz, with a signal amplitude of 10 mV. All measurements were carried out at laboratory temperature. EIS data were obtained after 5 min, 1 h, 2 h, 4 h, 8 h, 12 h, 24 h, 48 h, 72 h and 96 h of immersion (where possible). The measurement time of one experiment was 25.8 min. Electrochemical characteristics of prepared samples were compared to wrought magnesium with average grain size of 50 μm.

RESULTS

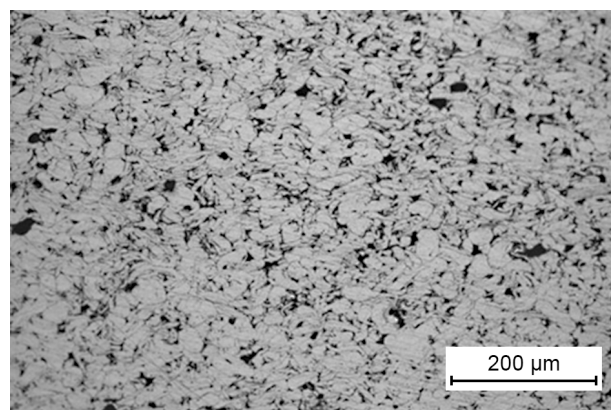
Microstructure

The microstructure of prepared samples obtained at different compacting pressures is shown in Fig. 2. Detail of the magnesium-based material microstructural evolution (powder particles deformation) due to the increased compaction pressure is obvious in Fig. 3. Samples prepared using 100 MPa as the compacting pressure were highly porous and only limited particle deformation was visible Fig. 2a and Fig 3a. The high porosity of the sample is observable also by the presence of the resin used for metallographic specimen molding on the polished and etched cross-section (Fig. 3a). Open porosity of approximately 20 % was calculated for the sample. Applying higher pressure than 100 MPa

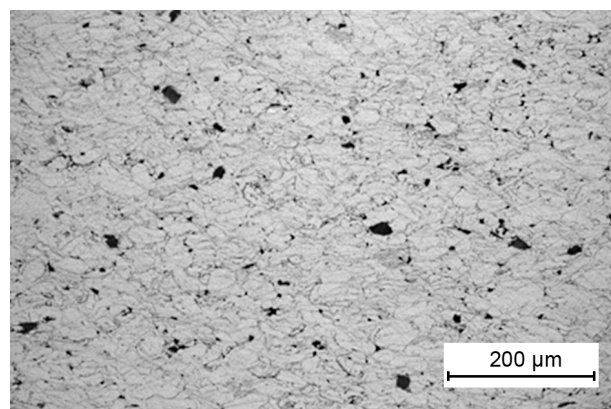
led to microstructural changes. A significant decrease in porosity and high plastic deformation of powder particles occurred at higher pressures. Using a pressure of 200 MPa resulted in powder particles plastic deformation due to the compaction and the porosity level decreased to approximately 10 %, Fig 2b. Compacting pressures of 300 MPa, 400 MPa and 500 MPa led to the



a) 100 MPa



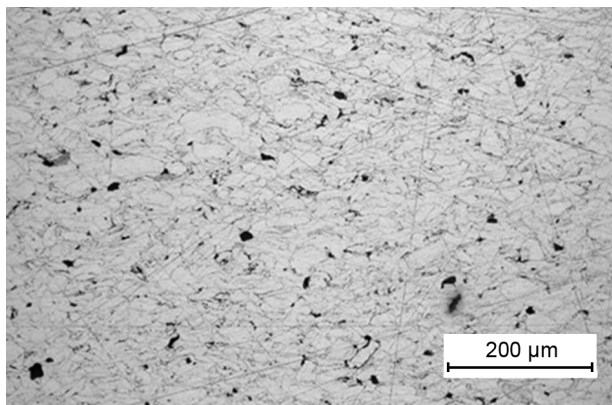
b) 200 MPa



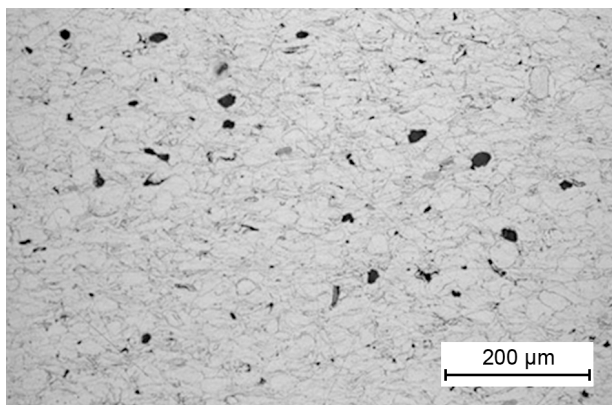
c) 300 MPa

Fig. 2. Evolution of microstructure of magnesium-based material prepared at different pressures, LM (continue on next page)

Obr. 2. Vývoj mikrostruktury hořčkových materiálů připravených při různých tlacích, LM (pokračování na další stránce)



d) 400 MPa



e) 500 MPa

Fig. 2. Evolution of microstructure of magnesium-based material prepared at different pressures, LM
 Obr. 2. Vývoj mikrostruktury hořčkových materiálů připravených při různých tlacích, LM

same microstructure with minimal differences in porosity (approximately 5 %) Fig. 2c, 2d and 2e respectively and Fig 3b, on this picture, small closed pores between powder grains are visible.

In Fig. 4 differences in compaction during sample preparation are represented. In the initial phase of compaction, the pressure increases very slowly, as particles reorganize to fill the free space between them. This almost linear increase in pressure is found under approximately 50 MPa, after this phase compacting pressure increases exponentially, as the plastic deformation takes place. Greatest change in compacting pressure lies in region between 100 MPa and 300 MPa. Curves of compacting pressure of 300 MPa, 400 MPa, and 500 MPa are again almost linear near the end of compacting, which means that only minimal changes in microstructure take place after 300 MPa compacting pressure, which is also visible in Fig. 2c, 2d, and 2e.

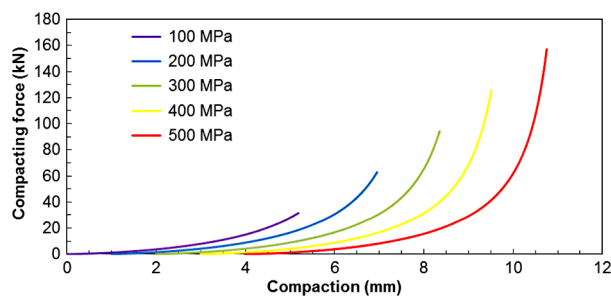
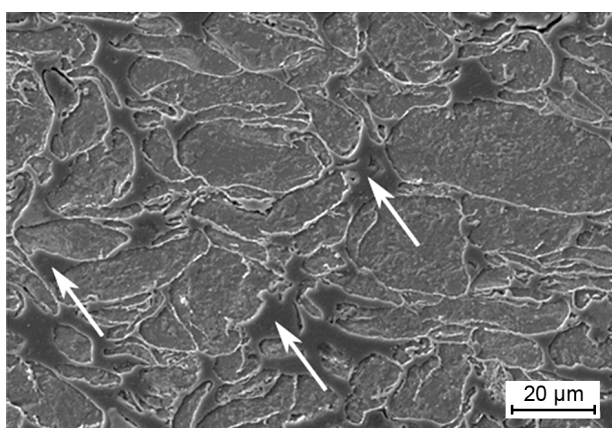
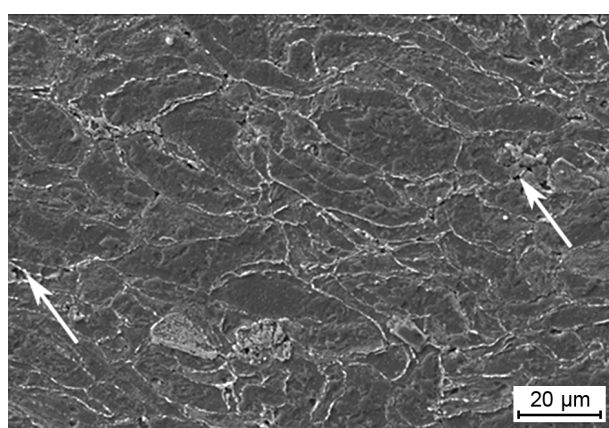


Fig. 4. Process of powder compaction, curves are shifted by 1 mm from each other for better visibility
 Obr. 4. Proces zhuňování prášků, křivky jsou od sebe posunuty o 1 mm pro lepší viditelnost



a) open porosity filled with resin / otevřená porozita s lisovací hmotou



b) closed porosity / uzavřená porozita

Fig. 3. Microstructure of samples prepared at different compaction pressures, SEM, 5 % Nital; marked areas: a) open porosity filled with resin, b) closed porosity
 Obr. 3. Mikrostruktura vzorků připravených při různých tlacích, SEM, 5% nital, označená místa: a) otevřená porozita s lisovací hmotou, b) uzavřená porozita

Electrochemical characterisation

EIS measurements were performed on magnesium samples compacted at 500 MPa and on wrought pure magnesium samples. Pure wrought magnesium was used as a basic material for obtained electrochemical characteristics comparison. Samples compacted at 500 MPa were chosen due to their microstructure characteristic with the lowest porosity from whole the prepared samples. Nyquist plots for cold compacted and wrought magnesium are shown in Figs. 5 and 6 respectively. Equivalent circuits used for the plots evaluation are shown in Fig. 7. Determined electrochemical characteristics are given in Tables 1 and 2.

Nyquist plots for compacted magnesium in 0.9 % NaCl solution are given in Fig. 5. Two different plot characters can be seen in the graph. In the beginning of the measurement two loops were observed on the curve; for the evaluation of the plot was used an equivalent circuit shown in Fig. 7c. Only one loop was measured

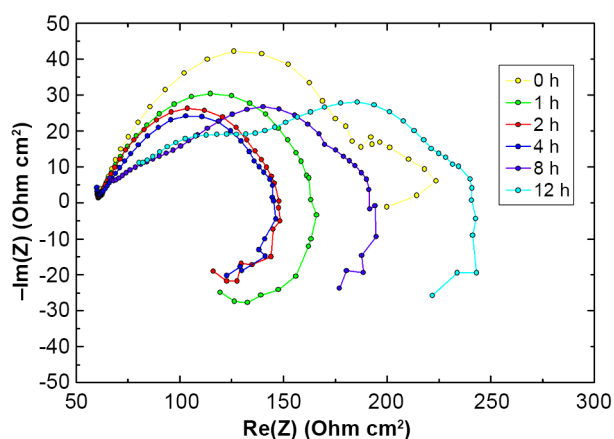


Fig. 5. Nyquist plots for cold compacted magnesium powder in 0.9 % NaCl
Obr. 5. Nyquistovy grafy pro hořčikový prášek zhutněný za studena v 0.9 % NaCl

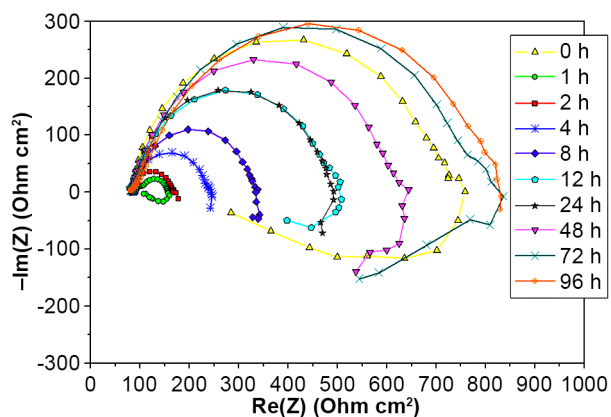


Fig. 6. Nyquist plots for wrought magnesium in 0.9 % NaCl
Obr. 6. Nyquistovy grafy pro tvářený hořčík v 0.9 % NaCl

in the case of compacted magnesium exposed to NaCl solution for the time longer than 1 h and the equivalent circuit shown in Fig. 7b was used for the obtained data evaluation. After 8 hours of exposure two loops in the Nyquist plots were observed again. The experiment was stopped after 12 hours of material exposure to the used solution due to the rapid degradation of the experimental material. Polarization resistance of the material, Table 1, at the beginning of the experiment was 192 $\Omega \text{ cm}^2$. Increasing the exposure time the value decreased to 86 $\Omega \text{ cm}^2$ at 4 hours of exposure. After 8 hours of exposure the polarization resistance increase and at 12 hours of exposure reached the value of 178 $\Omega \text{ cm}^2$.

Nyquist plots for wrought magnesium in 0.9 % NaCl solution are given in Fig. 6. In this case, three different Nyquist loops types were measured. The equivalent circuit of the Fig. 7b was chosen for the description of corrosion behavior in first 5 min of material exposure to the solution. At 1 h, the equivalent circuit of the Fig. 7c was used. In this case, one extra capacitance loop was present in the graph. Further, in the interval 2-8 h, the simplified Randles cell was used (Fig. 7a) to analyze the obtained data. After 12 h of exposure the inductive

Tab. 1. Summary of polarisation resistances of cold compacted magnesium / Shrnutí polarizačních odporů lisovaného hořčíku

Time [h]	R_s [$\Omega \text{ cm}^2$]	R_1 [$\Omega \text{ cm}^2$]	R_2 [$\Omega \text{ cm}^2$]	R_3 [$\Omega \text{ cm}^2$]	R_p [$\Omega \text{ cm}^2$]
0	61	77	94	21	192
1	61	49	57	–	107
2	61	45	43	–	88
4	62	49	37	–	86
8	63	44	23	50	134
12	61	59	103	16	178

Tab. 2. Summary of polarisation resistances of wrought magnesium / Shrnutí polarizačních odporů tvářeného hořčíku

Time [h]	R_s [$\Omega \text{ cm}^2$]	R_1 [$\Omega \text{ cm}^2$]	R_2 [$\Omega \text{ cm}^2$]	R_3 [$\Omega \text{ cm}^2$]	R_p [$\Omega \text{ cm}^2$]
0	82	312	324	–	635
1	88	34	15	18	68
2	84	81	–	–	81
4	86	150	–	–	150
8	89	240	–	–	240
12	91	282	122	–	404
24	84	401	54	–	455
48	86	223	315	–	539
72	91	438	270	–	708
96	95	739	–	–	739

behavior was found again and circuit from the Fig. 7b was used for data analysis. This corrosion behavior was observed until the end of the experiment. Polarization resistance determined at the beginning of the experiment significantly decreased from the first EIS measurement until one hour, Table 2. The polarization resistance grows gradually from the 1 h of the exposure to the end of the experiment. The maximum value of R_p was reached at the end of the experiment after 96 h, Table 2.

Three equivalent circuits were used for fitting of the obtained Nyquist plots. Firstly, it was simplified Randles circuit, Fig. 7a, where R_s represents solution resistance, Q represents capacitance of double layer formed on the specimen surface and R_p represents polarization resistance of formed double layer. Equivalent circuit shown in Fig 7b consists of solution resistance R_s , Q_1 is the capacitance of the present corrosion layer, R_1 is the resistance of the capacitance part. Another time-independent part of this circuit is the inductive loop with inductance L_2 and their resistance R_2 . The resulting polarization resistance R_p is the sum of R_1 and R_2 resistances. The last used equivalent circuit is in the Fig 7c. This equivalent circuit consists of three-time independent loops. There are two capacitance loops in high and low frequencies and one inductive

loop. The elements R_s is the solution resistance, Q_1 and R_1 are capacitance and resistance of corrosion products barrier, Q_2 and R_2 are capacitance and resistance of the inner porous layer. Elements of the inductive loop are inductance L and resistance of the inductor R_3 .

DISCUSSION

Microstructure and electrochemical characteristic of prepared magnesium-based materials were observed to be highly dependent on the applied compacting pressure. Samples prepared using 100 MPa as a compacting pressure showed minimum plastic deformation of powder particles, and the calculated porosity of these samples was approximately 20 %. This high porosity prohibited electrochemical measurements, as porosity this high is opened, therefore the electrolyte would flow through the sample. The high reactivity of magnesium would lead to fast material degradation.

Increasing compacting pressure to 200 MPa led to significant changes in microstructure, as plastic deformation of powder particles was more severe. The porosity of these samples dropped to approximately one-half of the values of previous samples (100 MPa), however, the porosity was still opened, and therefore the electrochemical measurements were still impossible to conduct. Calculated porosity level is similar to [12]. The greatest change in the material takes place during 100 MPa compaction because in this region loose powder is shaped into porous compacted material. Compacting pressure of 200 MPa yields observable changes in microstructure as the open porosity diminishes. Higher compacting pressures lead only to minimal changes in microstructure due to limited deformation possibilities of magnesium and absence of open porosity.

Using higher compaction pressure resulted in significant microstructural changes comparing to 200 MPa. Compacting pressures of 300 MPa, 400 MPa and 500 MPa resulted in similar microstructure and porosity. High compacting pressures led to severe plastic deformation of powder particles and decrease in porosity to approximately 5 %.

Behaviour of wrought magnesium after 5-minute immersion in the electrolyte (0.9% NaCl) was probably connected with the development of corrosion products on the sample surface. The presence of inductive loop is probably caused by either interaction of corrosion products or impurities with the basic material, where the corrosion products or impurities are nobler than the base, or by the presence of pitting corrosion [18, 19]. After 1 hour of exposure, the chosen equivalent circuit corresponds to the creation of porous corrosion barrier on the sample surface. Following exposure of the sample

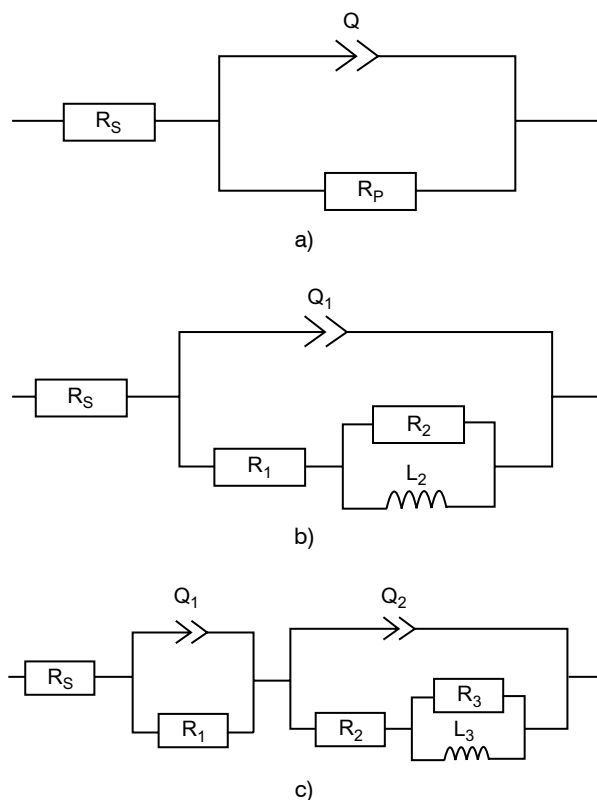


Fig. 7. Equivalent circuits used for the Nyquist plots evaluation

Obr. 7. Ekvivalentní obvody použité pro vyhodnocení Nyquistových grafů

surface to the electrolyte led to the additional creation of corrosion products on the sample surface. The stability of the corrosionprotecting layer was evident on the changed plots which led to using the simplified equivalent circuit. After 12 h of exposure, the corrosion behaviour of the wrought material changed again, an inductive loop was present due to partial damage to the protecting corrosion layer [20].

A similar evolution of the corrosion process was observed in the case of compressed material, however, less pronounced protecting against further material degradation was observed due to the surface oxidation, which prohibited magnesium particles full compaction, providing a porous layer through which the electrolyte progress further into the material. This could be connected with still present porosity, where the pores can act as corrosion initiation sites [19]. The physical meaning of this fact can be interpreted as electrolyte penetration into inner porous structure and creation of microcells due to ions concentration gradient (inductive loop) and formation of a double layer on the specimen substrate (capacitance loop). The response from the inner porous layer is not clear.

Based on the Nyquist plots the corrosion mechanism of the compacted magnesium can be described as follows. After 5 min exposure, an corrosion protective layer started to create, however, the layer was porous. Following exposure of the material to the corrosive environment led to the creation of protective layer, more compact comparing to the beginning of the measurements. After 8 h of exposure partial damage of corrosion layer occurred, this leads to measurement of one more capacitance loop. This phenomenon can be interpreted as a creation of two double layers, one between the solution and corrosion layer and other between corrosion layer and specimen surface.

Cold compacted materials significantly differ from wrought magnesium both from the point of microstructure and electrochemistry. The models of equivalent circuits are similar, however, their physical meaning differs. Generally, inductive loops, in the case of wrought magnesium, correspond with possible pitting corrosion mechanism or galvanic microcell creation between more noble corrosion products and magnesium [18, 19]. In the case of cold compacted magnesium, the origin of inductive loops may correspond to ion concentration gradient in the porous structure, however, these two mechanisms cannot be distinguished using EIS method. From the corrosion point of view wrought magnesium exhibits higher polarization resistance than cold compacted magnesium. This is probably due to the presence of pores in the cold compressed magnesium microstructure enlarging the real sample surface, acting as a corrosion attack places and complicate the protecting corrosion layer creation.

CONCLUSION

Samples with different microstructure and porosity were prepared using uniaxial cold compaction process by the application of different pressures. Electrochemical corrosion characteristics of samples prepared using 500 MPa were compared with those of wrought pure magnesium.

Influence of compacting pressure on the resulting microstructure and electrochemical characteristics are listed below:

- Compacting pressure has a significant influence on prepared bulk microstructure. Compacting pressure of 100 MPa led to minimal plastic deformation of powder particles and the highest porosity (20 %). Powder particles deformation increased and porosity decreased with increasing compacting pressure. Applying compacting pressure in the range from 300 to 500 MPa led to similar microstructure and porosity of obtained samples.
- EIS measurement revealed lower polarization resistance of compacted magnesium when compared to the wrought material. On the beginning of the exposure, the compacted material reached a value of the polarization resistance three times lower when compared to the wrought magnesium. The R_p , obtained for the compacted magnesium at 12 hours of the exposure to the corrosion environment, reached only less than a half of the value obtained for wrought material and the corrosion process was so pronounced, that the experiment had to be stopped.
- Differences in electrochemical corrosion characteristic were probably caused by the presence of pores in cold compacted magnesium microstructure, therefore larger exposed free surface was subjected to the corrosion environment. Also, a different mechanism of corrosion process can be connected with different behavior of two examined magnesium states.

Acknowledgements

This work was supported by project Nr. LO1211, Materials Research Centre at FCH BUT- Sustainability and Development (National Programme for Sustainability I, Ministry of Education, Youth and Sports)

REFERENCES

1. Witte, F., The history of biodegradable magnesium implants: A review. *Acta Biomaterialia*. **2010**, 1680-1692.
2. Al-Zubaydi, A., et al. Superplastic behaviour of AZ91 magnesium alloy processed by high-pressure torsion. *Materials Science and Engineering A* **2015**, 637(1-2), 1-11.

3. Lee, H., et al. Evolution in hardness and texture of a ZK60A magnesium alloy processed by high-pressure torsion. *Materials Science and Engineering A* **2015**, 630, 90-98.
4. Suwas, S., Gottstein, S., Kumar, R., Evolution of crystallographic texture during equal channel angular extrusion (ECAE) and its effects on secondary processing of magnesium. *Materials Science and Engineering* **2007**, 471 (1-2), 1-14.
5. Zhao, Y.F., et al. High strength Mg–Zn–Ca alloys prepared by atomization and hot pressing process. *Materials Letters* **2014**, 118, 55-58.
6. Campo, R., et al, a další. Mechanical properties and corrosion behavior of Mg-HAP composites. *Journal of the Mechanical Behavior of Biomedical Materials*. **2014**.
7. Zheng, Y.F., et al. In vitro degradation and cytotoxicity of Mg/Ca composites produced by powder metallurgy. *Acta Biomaterialia*. **2010**, 6 (5), 1783-1791.
8. Kang, M., et al. Production and bio-corrosion resistance of porous magnesium with hydroxyapatite coating for biomedical applications. *Materials Letters* **2013**, 108, 122-124.
9. Anish, R., Sivapragash, M., A Robertsingh, G. Compressive behaviour of SiC/nsc reinforced Mg composite processed through powder metallurgy route. *Materials* **2014**, 63, 384-388.
10. Zhong, X.L., Wong, W.L.E., Gupta, M. Enhancing strength and ductility of magnesium by integrating it with aluminum nanoparticles. *Acta Materialia* **2007**, 55 (18), 6338-6344.
11. Liao, J., Hotta, M., Mori, Y. Improved corrosion resistance of a high-strength Mg–Al–Mn–Ca magnesium alloy made by rapid solidification powder metallurgy. *Materials Science and Engineering A* **2012**, 544, 10-20.
12. Čapek, J., Vojtěch, D. Effect of sintering conditions on the microstructural and mechanical characteristics of porous magnesium materials prepared by powder metallurgy. *Materials Science and Engineering C* **2014**, 35, 21-28.
13. Čapek, J., Vojtěch, D., Properties of porous magnesium prepared by powder metallurgy. *Materials Science and Engineering C* **2013**, 33 (1), 564-569.
14. Bi, Y., Zheng, Y., Li, Y. Microstructure and mechanical properties of sintered porous magnesium using polymethyl methacrylate as the space holder. *Materials Letters* **2015**, 161, 583-586.
15. Rashad, M., et al. Improved mechanical proprieties of “magnesium based composites” with titanium–aluminum hybrids. *Journal of Magnesium and Alloys* **2015**, 3 (1), 1-9.
16. I. Baker, D. Iliescu A Y. Liao. Containerless Consolidation of Mg Powders Using ECAE. *Materials and Manufacturing Processes* **2010**, 25(12), 1381.
17. M.D. Pereda et al. Corrosion inhibition of powder metallurgy Mg by fluoride treatments. *Acta Biomaterialia* **2010**, 6(5), 1772-1782.
18. M. Bukovina and B. Hadzima, “vplyv úpravy povrchu na elektrochemické charakteristiky horčikovej zliatiny AE21”, *Transfer inovácií* **2009**, 15, 28-32.
19. G. Song, Corrosion of magnesium alloys, 1.. Philadelphia, PA: Woodhead Publishing, **2011**.
20. B. Setzler and T. Fuller, “A Physics-Based Impedance Model of Proton Exchange Membrane Fuel Cells Exhibiting Low-Frequency Inductive Loops”, *Journal of the Electrochemical Society* **2015**, 162 (6), F519-F530.